Carbohydrate Polymers 83 (2011) 1937–1946

Contents lists available at ScienceDirect

Carbohydrate Polymers

journal homepage: www.elsevier.com/locate/carbpol

Impacts of nanowhisker on formation kinetics and properties of all-cellulose composite gels

Yixiang Wang, Lingyun Chen*

Department of Agricultural, Food and Nutritional Science, University of Albeta, Edmonton, AB, Canada T6G 2P5

ARTICLE INFO

Article history:
Received 16 August 2010
Received in revised form 26 October 2010
Accepted 27 October 2010
Available online 3 November 2010

Keywords:
Cellulose nanowhiskers
All-cellulose hydrogels
Reinforcement
Membrane–matrix hybrid systems
Drug delivery

ABSTRACT

Composite gels, with cellulose nanowhiskers as the reinforcing phase and regenerated cellulose as the matrix, were firstly developed by a rapid thermal-induced phase separation followed by a regenerating process. The gelation behavior, regeneration kinetics, morphology and properties of the all-cellulose composite gel system were investigated by advanced rheometer, potentiometric titration, scanning electron microscopy, Fourier-transform infrared spectroscopy, texture analyzer and swelling testing in the presence of different amount of cellulose nanowhiskers. The results revealed that cellulose nanowhiskers could act as the "bridge" to facilitate the crosslinking of cellulose chains during gel formation process. Moreover, they can significantly improve the dimensional stability and mechanical strength of the regenerated gels. *In vitro* experiment demonstrated that these gels, featuring membrane–matrix hybrid structures, could be used for controlled release of macromolecules in the simulated body fluid.

1. Introduction

Polymeric hydrogels have been used extensively in the development of bioengineering and biomedical applications such as tissue engineering scaffolds and drug delivery formulations (Nguyen & West, 2002). Those based on natural polymers with physical crosslinks are especially interesting because of their unique advantages of abundance, nontoxicity, biocompatibility and biodegradability (Liang, Wu, Tian, Zhang, & Xu, 2008). Cellulose, which is considered as an almost inexhaustible source of raw material, has been formed into fibers, films, gels, micro- and nano-particles for different applications (Cai et al., 2007; Klemm, Heublein, Fink, & Bohn, 2005; Luo, Liu, Zhou, & Zhang, 2009; Zhou, Chang, Zhang, & Zhang, 2007). Cellulose hydrogels can be obtained by chemical crosslinking of water-soluble cellulose derivatives, such as cellulose acetate, hydroxyethylcellulose and sodium carboxymethylcellulose (Andrews, Gorman, & Jones, 2005; Entcheva et al., 2004; Fundueanu et al., 2005). Physically crosslinked cellulose hydrogels are recently prepared by developing intermolecular hydrogen bonds via hydroxyl groups on cellulose molecular chains (Bingöl, Strandberg, Szabo, & Wegner, 2008; Hoepfner, Ratke, & Milow, 2008; Klemm, Schumann, Udhardt, & Marsch, 2001). The formation of such gel systems involves two steps: pre-gelation and regeneration. Chang, Lue, and Zhang (2008) prepared cellulose/poly(vinyl alcohol) hydrogels from NaOH/urea aqueous solution by applying a pre-gelation process of freezing and thawing for 98 h. Liang, Zhang, Li, & Xu (2007) stored cellulose/NaOH/thiourea aqueous solution at pre-gelation temperatures of 5, 20, and 35 °C for three weeks to obtain cellulose physical gel with dense structure. Gavillon & Budtova (2007) kept cellulose/NaOH aqueous solution at room temperature for 15 h to prepare the pre-gelated cellulose gel and subsequently investigated the regeneration kinetics of cellulose gels immersed in a nonsolvent bath. In spite of success to make gels with good mechanical strength, solute permeability and nontoxicity (Wu et al., 2010), these methods generally include a time-consuming pre-gelation process, which is not practical for industrial production.

Our preliminary experiment showed that a mild thermal treatment can provide a convenient and rapid method to prepare irreversible physically crosslinked cellulose gels from a NaOH–urea aqueous system. However, an obvious irregular shrinkage took place when these cellulose gels were immersed and regenerated in a water bath (Sescousse & Budtova, 2009), leading to the distortion of the final products. Thus, it will be interesting to introduce fillers to reinforce the physically crosslinked cellulose networks.

Cellulose nanowhiskers, rod-like nanocrystals with highly mechanical performance obtained from a range of renewable biosources, have been successfully used as reinforcing fillers in a series of synthetic and natural polymeric matrices (Chen, Liu, Chang, Cao, & Anderson, 2009; Lu, Weng, & Cao, 2006; Paralikar, Simonsen, & Lombardi, 2008; Roohani et al., 2008). These nanowhiskers have a high tendency to form networks via surface hydroxyl group,

* Corresponding author. Tel.: +1 780 492 0038; fax: +1 780 492 4265.
E-mail address: lingyun.chen@ualberta.ca (L. Chen).

0144-8617/$ – see front matter © 2010 Elsevier Ltd. All rights reserved.
doi:10.1016/j.carbpol.2010.10.071

which is advantageous for the formation of load-bearing percolating architectures within the host polymer matrix because the stress transfer can be facilitated by hydrogen bonding between the nanowhiskers (Capadona et al., 2009). Since the cellulose nanowhisker fillers can also develop hydrogen bonds with the host polymer matrix, they may impact the gel formation and properties in addition to mechanical strength. Understanding of such impacts is essential to design novel gels with desirable applications. However, research effort in this area is limited. Using cellulose nanowhiskers to reinforce cellulose hydrogels has never been reported previously.

We reported here a convenient method to prepare nanowhisker-reinforced, all-cellulose composite gels with the intention of developing a novel high-performance porous material for potential biomedical applications. Cellulose nanowhiskers with high molecular weight were dispersed in the cellulose–NaOH–urea aqueous system, which could only dissolve cellulose with molecular weight below 1×10^5. The impacts of cellulose nanowhiskers on the gelation behaviors, regeneration kinetics, morphologies and properties of the gels were carefully investigated. Moreover, the gel controlled release properties were studied in the simulated physiological conditions using bovine serum albumin (BSA) as a model molecule.

2. Experimental

2.1. Materials

Two kinds of cellulose (cotton linter pulp) were provided by Hubei Chemical Fiber Group Ltd. (Hubei, China). Their viscosity-average molecular weight (M_η) was determined by using an Ubbelohde viscometer in LiOH/urea aqueous solution at $25 \pm 0.05\,^\circ$C and calculated according to the Mark-Houwink equation to be 3.0×10^5 and 1.0×10^5, respectively (Cai, Liu, & Zhang, 2006). Bovine serum albumin (BSA, Fraction V) were purchased from Sigma–Aldrich (MO, USA). All other chemical reagents were purchased from Fisher Scientific (Ontario, Canada) and were used as received unless otherwise described.

2.2. Preparation of cellulose nanowhiskers

Cellulose with high molecular weight was dispersed in sulfuric acid, and the mixture was added to a three-necked flask equipped with a mechanical stirrer and a thermometer. The flask was placed into a water bath and stirred vigorously. The suspension was then diluted with distilled water, and centrifuged at 8000 rpm (Avanti® J-E centrifuge, Beckman Coulter, USA) for 15 min. The process was repeated three times and the resulting suspension was dialyzed until the pH reached 4. Finally, the dispersion was freeze-dried to obtain cellulose nanowhisker powder (CN). The average length (L) and width (D) of CNs observed by atomic force microscopy (AFM, Molecular Imaging, Arizona, USA) were estimated to be 300 and 21 nm, respectively (Wang, Chang, & Zhang, 2010).

2.3. Preparation of all-cellulose composite gels

The gel formation involved three steps: preparation of cellulose suspension, fabrication of physically crosslinked gels through thermal-induced phase separation, and regeneration of cellulose gels. Briefly, a 100 g mixture of NaOH, urea, and distilled water (7:12:81 by weight) was pre-cooled to $-12.6\,^\circ$C, and 4 g of cellulose with low molecular weight was added immediately with vigorous stirring for 5 min to obtain a transparent solution. After warming to room temperature, a desired amount of CN was added to the solution and stirred for 30 min. The suspension was centrifuged at 3000 rpm and $10\,^\circ$C for 5 min to remove air bubbles, and then injected into a plastic tube. The sealed tubes were kept in water bath at $40\,^\circ$C for 30 min to obtain physically crosslinked gels. Then the gels were removed from the tubes and regenerated in running water for 24 h. These all-cellulose composites were coded as CC0, CC20, CC35 and CC50, corresponding to a CN content (based on the total solid content) of 0, 20, 35 and 50 wt%, respectively.

2.4. Gels formation kinetics study

To understand the variation of the structures of all-cellulose composites during the thermal-induced phase separation and regeneration processes, the dynamic rheology experiment was carried out on an ARES-2000 rheometer (TA Instruments, DE, USA). Parallel plate geometry with a gap of 1 mm was used to measure dynamic viscoelastic parameters such as the shear storage modulus (G') and loss modulus (G'') as functions of angular frequency (ω), temperature (T), or time (t). The values of the strain amplitude were monitored to ensure that all measurements were set as 10%, which is within a linear viscoelastic regime. For each measurement, a fresh sample was used without pre-shearing or oscillating. To prevent dehydration during rheological measurements, a thin layer of low-viscosity paraffin oil was spread on the exposed surface of the measured suspension. For the frequency and time sweep measurements, time $t = 0$ min was defined when the temperature reached the desired value. The sweep of the frequency was from 0.1 to 100 rad/s. The dynamic temperature sweep measurements were conducted from 20 to $50\,^\circ$C at an angular frequency of 1 Hz and with heating rates of $2\,^\circ$C/min. The gelation behavior was studied at $40\,^\circ$C as a function of time at a constant frequency of 1 Hz.

The diffusion of NaOH, urea and water took place when all-cellulose gels were immersed in the regenerating bath. To achieve a better understanding of the regeneration kinetics, the evolution of NaOH concentration in the water bath as a function of time was measured using titration with acetic acid in the presence of an indicator as described by Gavillon et al. (Gavillon & Budtova, 2007). The proportion between sample/bath weights was 1/400, and magnetic stirrer with a low stirring rate (300 rpm) was used for bath homogenization. The amount of NaOH released from the sample in time was calculated knowing the initial sample and bath weights.

2.5. Gels structure characterizations

The morphology observation of the regenerated gels was carried out with a Hitachi X-650 scanning electron microscopy (SEM, Hitachi, Japan). The samples were frozen in liquid nitrogen and snapped immediately, and freeze-dried before SEM observation. The cross-sections and surfaces of the gels were sputtered with gold, observed and photographed. The cellulose crystalline structure and interaction in the regenerated gels were studied with an FTIR (Perkin Elmer Spectrum one, Wellesley, MA, USA) spectrophotometer in the region of 400–4000 cm^{-1}. The freeze-dried gels and CN powder were analyzed in KBr discs.

2.6. Mechanical property determinations

The mechanical properties of the composite gels were analyzed by a texture analyzer (Texture Technologies Corp., New York, USA). The gels with a cylindrical shape, i.e. ~10 mm in diameter and ~7 mm in height, were compressed at room temperature in air at a rate of 1 mm/min to evaluate their mechanical property. Raw data (force *vs* displacement) were converted to engineering stress and strain by the use of the initial dimensions of the gels.

2.7. Swelling measurements

The swelling ratio of the regenerated gels with different CN contents was analyzed with a gravimetric method in the distilled water at 25 °C. After the surfaces of the gels had been wiped with filter papers to remove excess water, the weights of the hydrogels were recorded. The equilibrium swelling ratio (*ESR*) was calculated as

$$ESR = \frac{W_s}{W_d} \quad (1)$$

where W_s is the weight of the regenerated gel at 25 °C, and W_d is the weight of the gel at dry state. To clarify the re-swelling, the freeze-dried hydrogel samples were again immersed in distilled water to rehydrate at 25 °C for 24 h. The results were expressed as water reuptake (*WR*), and can be calculated by

$$WR = \frac{W_r - W_d}{W_s - W_d} \times 100 \quad (2)$$

where W_r is the weight of the re-swelling gel, and other symbols are the same as defined above.

2.8. Release property investigation

The typical drug loading and in vitro drug release experiment were performed as follows: BSA was selected as model molecule to investigate the gel release properties. Simulated body fluid (SBF) was employed as the media and prepared by dissolving the following reagents in 1 L of ion-exchanged and distilled water (Kokubo & Takadama, 2006): NaCl = 8.035 g, $NaHCO_3$ = 0.355 g, KCl = 0.225 g, $K_2HPO_4{\cdot}3H_2O$ = 0.231 g, $MgCl_2{\cdot}6H_2O$ = 0.311 g, 1.0 M-HCl = 39 mL, $CaCl_2$ = 0.292 g, Na_2SO_4 = 0.072 g, Tris = 6.118 g. Swelled cylindrical cellulose gels (~0.5 g) were immersed entirely in 20 mg mL^{-1} BSA SBF solutions and incubated in sealed vessels at 0 °C for 24 h. The drug loading content (*LC*) was calculated by the following equation:

$$LC = \frac{W_{ld}}{W_s} \quad (3)$$

where W_{ld} is the weight of the loaded drugs in the regenerated gels.

Then, drug loaded gels were separated, wiped with filter papers to remove excess solution, and kept in 200 mL of SBF at 37 °C with shaking at a constant rate. The release medium (1 mL) solution was taken out for analysis at given time intervals and replaced with the same volume of fresh preheated SBF (37 °C). The extracted medium solution was analyzed by V-530 UV–vis spectrophotometer (Jasco Inc., MD, USA) at a wavelength of 280 nm. The release data were fitted to the following equations using regression analysis:

$$\text{Zero-order equation} \quad \frac{dM_t}{dt} = k, \quad (4)$$

where k is the constant, t is time, and M_t is the amount of drug released at time t.

$$\text{First-order equation} \quad \frac{dM_t}{dt} = k(M_0 - M_t), \quad (5)$$

where k is the constant, t is time, M_0 and M_t are the amounts of drug released at time 0 and t.

$$\text{Fickian model} \quad \frac{M_t}{M_\infty} = kt^{0.5} \quad (6)$$

where M_t/M_∞ is the fraction of drug released after time t relative to the amount of drug released at infinite time.

3. Results and discussion

3.1. Impact of nanowhisker on all-cellulose composite gels formation kinetics

The preparation of all-cellulose composite gels was divided into three steps to detailedly investigate the effects of CN content on the gel formation kinetics. Firstly, CNs were dispersed in the cellulose–NaOH–urea aqueous solution to form an even suspension. This suspension was then heated in the second step to form physically crosslinked gels through the thermal-induced phase separation process. In the third step, the resulted gels were regenerated by removing the solvent molecules to induce a further phase transition.

3.1.1. CN dispersion in cellulose solution

The rheological behaviors of cellulose composites changed distinctly during these three steps. Thus, an advanced rheometer was used to track the transitions and understand the effects of CN on the gel formation and properties. Fig. 1a shows the G' and G'' curves as a function of angular frequency for the cellulose solution with different CN contents. For all the samples, G' value was smaller than that of G'' in the range of measured frequencies, exhibiting a viscous liquid-like behavior with G' and G'' scaling approximately with ω by $G' \sim G'' \sim \omega$ (Cai & Zhang, 2006b). It has been suggested that the urea hydrates could be self-assembled at the surface of the NaOH hydrogen-bonded cellulose to form an inclusion complex (IC), leading to the dissolution of cellulose (Cai & Zhang, 2005). So, it is possible that a competitive binding also formed between CNs and solvent molecules which "switched off" the inter-particle hydrogen bonding interactions between CNs. Both G' and G'' values increased and the difference between these values became smaller when CN content increased. Similar results were reported in the multiwalled carbon nanotube/ionic liquid AmimCl mixtures, which indicated the strong interactions between the well-dispersed nanotubes and ionic liquids (Zhang et al., 2007). Therefore, it can be deduced that, in our systems, the same strong interactions existed between CNs and solvent molecules to keep CNs at a "switched off" status. This is important because the extent of the reinforcement of nanowhiskers depends on their dispersion in the matrix and the generation of a strong filler–matrix interface through physic-chemical bonding (Wang & Zhang, 2008). Since cellulose nanowhiskers have a strong tendency for aggregation via hydrogen bonds to decrease the reinforcing effect (Capadona et al., 2007, 2009), it is essential to break the hydrogen bonding interactions during the processing to ensure cellulose nanowhiskers can be uniformly dispersed in the matrix (Capadona, Shanmuganathan, Tyler, Rowan, & Weder, 2008; Qi, Cai, Zhang, & Kuga, 2009; Shanmuganathan, Capadona, Rowan, & Weder, 2010).

3.1.2. Thermal-induced physical crosslinking

The formation of physically crosslinked gels triggered by thermal treatment was also monitored by rheometer (Fig. 1b and c). The crossover of G' and G'' curves was chosen as a qualitative indicator of the gel point, which only showed the transition current under external factors' influences (Sahiner, Singh, Kee, John, & McPherson, 2006). It should be pointed out that the gel point determined by this method is frequency dependent (Ruan, Lue, & Zhang, 2008), and the frequency of 1 Hz was fixed in our tests. For all the samples, G' and G'' curves were parallel when the temperature was below 30 °C, indicating the suspensions were rather stable. Above 30 °C, G' value increased dramatically and a crosspoint of G' and G'' curves appeared, suggesting the formation of an elastic gel network. It is well known that the strength of hydrogen bonding is dependent on temperature. The elevation of the temperature led to the weakened hydrogen bond strength between cellulose and sol-

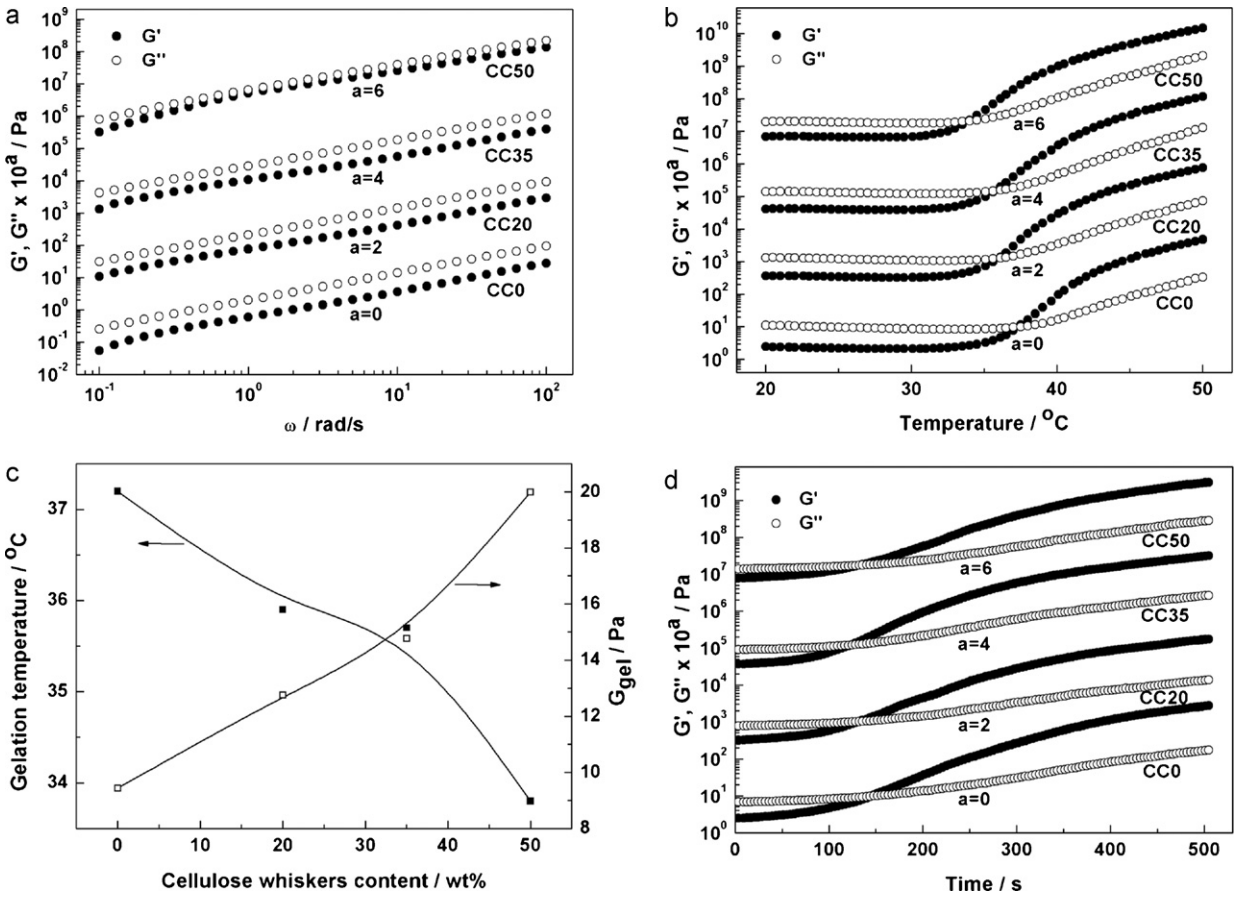

Fig. 1. (a) Angular frequency dependence of storage modulus (G', ●) and loss modulus (G'', ○) of composite cellulose solutions at 25 °C. (b) Temperature dependence of storage modulus (G', ●) and loss modulus (G'', ○) of composite cellulose solutions with a heating rate of 2 °C/min at a frequency of 1 Hz. (c) Gelation temperature and G_{gel} as a function of cellulose nanowhiskers content. (d) Time dependence of storage modulus (G', ●) and loss modulus (G'', ○) of composite cellulose solutions at 40 °C and a frequency of 1 Hz. The data are shifted along the vertical axis by 10^a with the given a value to avoid overlapping.

vent molecules, whereas the intra- and intermolecular hydrogen bonds of cellulose tended to increase as a result of its strong self-association tendency (Cai & Zhang, 2006b). Therefore, the structure of inclusion complexes were destroyed and physical entanglements occurred between the cellulose backbones when the temperature was above 30 °C (Weng, Zhang, Ruan, Shi, & Xu, 2004). This is called a thermal-induced phase separation processing. During the sol–gel transition, the hydrogen bonding interactions between the cellulose molecules were "switched on". With the increase of CN contents, the gelation temperature decreased from 37.2 to 33.8 °C and the gel modulus (G_{gel}) raised from 9.4 to 20.0 Pa, as shown in Fig. 1c, suggesting that CNs played an important role to facilitate the crosslinking of cellulose molecules. The similar effects were also observed in the waterborne polyurethane matrix by forming hydrogen bonding interactions (Wang, Tian, & Zhang, 2010). This was further confirmed by the results in Fig. 1d which shows the time dependence of G' and G'' curves of cellulose solutions with different CN contents at 40 °C. The gelation of the all-cellulose suspensions took place easily (within 150 s). With the addition of CNs, the gelation time decreased from 143.9 to 124.4 s. It was assumed that a more jammed cellulose suspension was formed when CN content was high, so that the distances among cellulose molecules were greatly shortened. Thus, when the temperature was raised to 40 °C to destroy the inclusion complexes, the hydrogen-bonding interactions among cellulose chains were "switched on" more easily and rapidly. Moreover, the rod-like CNs could act as the "bridges" to mediate between the cellulose chains by developing cellulose-CN hydrogen bonds at the "switching on" status to promote the gelation process and support the gel network.

3.1.3. All-cellulose gel regeneration

During the regeneration process, the solvent is replaced by a cellulose nonsolvent which should be miscible with the aqueous NaOH-urea solution to trigger a phase separation. Water was chosen as the nonsolvent to avoid the usage of organic solvents in this study. Fig. 2a shows the mechanical property of cellulose gels before and after regeneration. Before the regeneration, cellulose molecules and CNs were combined together through hydrogen bonds. The G' curves of these samples presented a plateau-like behavior at lower frequencies. CNs acted as the crosslinking points, and the height and width of the plateau increased with CN content, indicating that the hydrogen bonded network became stronger and more elastic. The G' curve of CC50 was flat and much higher than other curves, which was the result of the extremely jammed network caused by the high CN content. When the thermal-induced gels were immersed in the water bath, another phase separation took place, resulting in a further cellulose molecular chain entanglement and the formation of new cellulose crystalline regions (Qi et al., 2009). Therefore, the plateaus of G' curves raised approximate three orders of magnitude after regeneration. Interestingly, an obvious reinforcing effect was still observed in the all-cellulose composite gels, which suggested the strong reinforcement of CNs even in a tough matrix.

The photographs of CC0 and CC50 before and after regeneration in water are shown in Fig. 2. Before the regeneration, CC0 exhib-

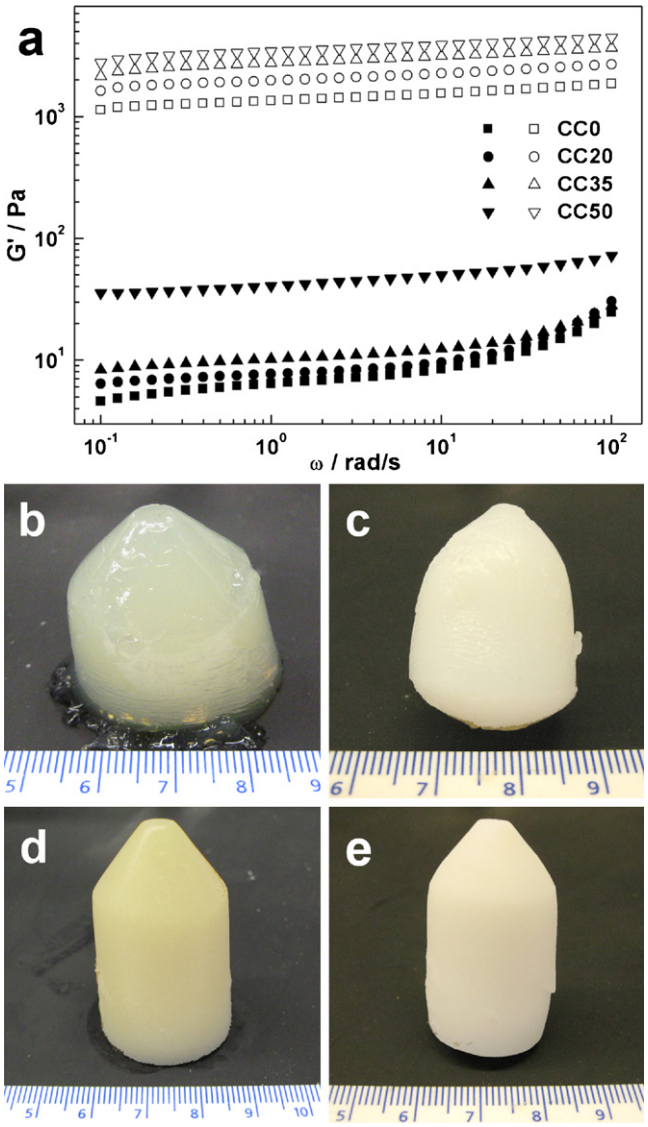

Fig. 2. (a) Angular frequency dependence of storage modulus (G') of cellulose gels having different cellulose nanowhiskers contents before (solid symbols) and after (open symbols) regeneration in water at 25 °C. Photographs of all-cellulose gels before (left) and after (right) regeneration in water at 25 °C with different cellulose nanowhiskers contents: 0 (b, c) and 50 wt% (d, e).

ited a weak character with an unstable shape, whereas CC50 acted like elastic foam with well-formed dimensions. It is suggested that gel mechanical property was significantly improved by addition of CNs, which made the all-cellulose gels more processable. An irregular shrinkage of CC0 occurred during gel regeneration process as shown in Fig. 2c. That was because the shrinking rate of every part on the gel was different, so as to distort the regenerated gel. However, CC50 exhibited a similar shape before and after regeneration. It was worth noting that CC20 and CC35 also exhibited well-formed dimensions and the extent of shrinkage decreased when CN content increased from 0 to 50 wt%. It could be explained that abundant hydrogen bonding interactions were "switched on" between CNs and cellulose molecules, which formed a strong and elastic network to support and diffuse the stress faster and uniformly, leading to the homogeneous shrinkage. Therefore, it is easy to control the shape of the regenerated products and a uniform inside porous structure can be expected in the CN filled cellulose gels.

The kinetics of cellulose regeneration in the presence of the different content of CN was investigated by measuring the evo-

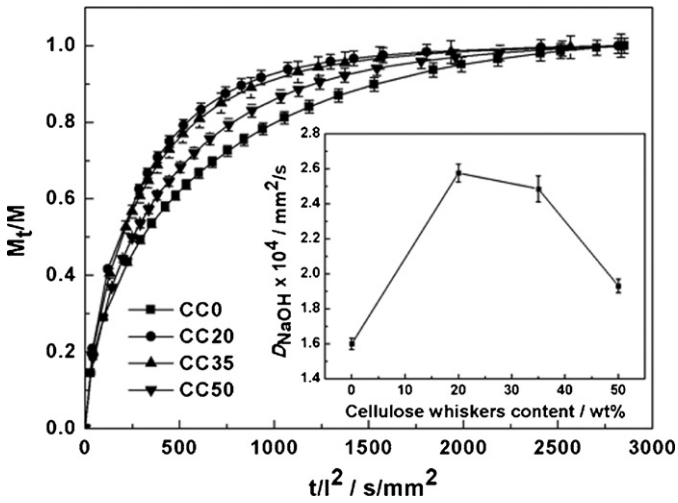

Fig. 3. Diffusion of NaOH from cellulose gels having different cellulose nanowhiskers contents into the water regenerating bath at 25 °C. *Inset*: Dependence of NaOH diffusion coefficient on cellulose nanowhiskers contents in a water bath at 25 °C.

lution of NaOH concentration in the water bath. The diffusion of NaOH as a function of time is shown in Fig. 3. Fickian diffusion mechanism was employed to fit the experimental data. It is widely applied in drug release from the polymeric matrix and to study the formation of membranes due to phase separation (Singh, 2007), and was already used to describe the kinetics of cellulose regeneration from cellulose-*N*-methylmorpholine-*N*-oxide-water and cellulose-NaOH-water solutions (Biganska & Navard, 2005; Sescousse & Budtova, 2009). Fickian model is calculated from the following equations:

Early-time approximation ($0 \le M_t/M_\infty < 0.5$):

$$\frac{M_t}{M_\infty} = 4\left(\frac{Dt}{\pi l^2}\right)^{1/2} \tag{7}$$

Half-time approximation ($M_t/M_\infty = 0.5$):

$$D = 0.049/(t/l^2)_{1/2} \tag{8}$$

Late-time approximation ($0.5 < M_t/M_\infty \le 1$):

$$\frac{M_t}{M_\infty} = 1 - \frac{8}{\pi^2}\exp\left(\frac{-\pi^2 Dt}{l^2}\right) \tag{9}$$

where (M_t/M_∞) is the fractional release, M_t and M_∞ are the amounts released at time t and equilibrium, respectively, D is the diffusion coefficient and l is half of the thickness of the sample. The diffusion profiles of NaOH were well fitted with early-, half-, and late-time approaches ($R^2 = 0.99$), indicating the validity of the Fickian approach for the all-cellulose composite gels. The diffusion coefficient was calculated by the half-time approximation and plotted in the insert of Fig. 3. The diffusion behavior of the NaOH from the gel matrices was mainly controlled by "porous membrane" because a relatively lower diffusion coefficient was observed (Sescousse & Budtova, 2009). However, CC0 displayed a lowest diffusion coefficient (1.60×10^{-4} mm^2/s), while the diffusion coefficient increased to the maximum (2.58×10^{-4} mm^2/s) in CC20 and then decreased with the further addition of CNs. It is interesting to notice that, besides the "porous membrane", the inside structure of the all-cellulose composite gels may also contribute to the regenerating process, and a stable and well-supported architecture was propitious to the diffusion of NaOH and water molecules, leading to the high regenerating rates of CC20 and CC35. While with increase of the CNs content, the more jammed hydrogen bonded network were formed which lower the diffusion rate of NaOH, resulting in an obvi-

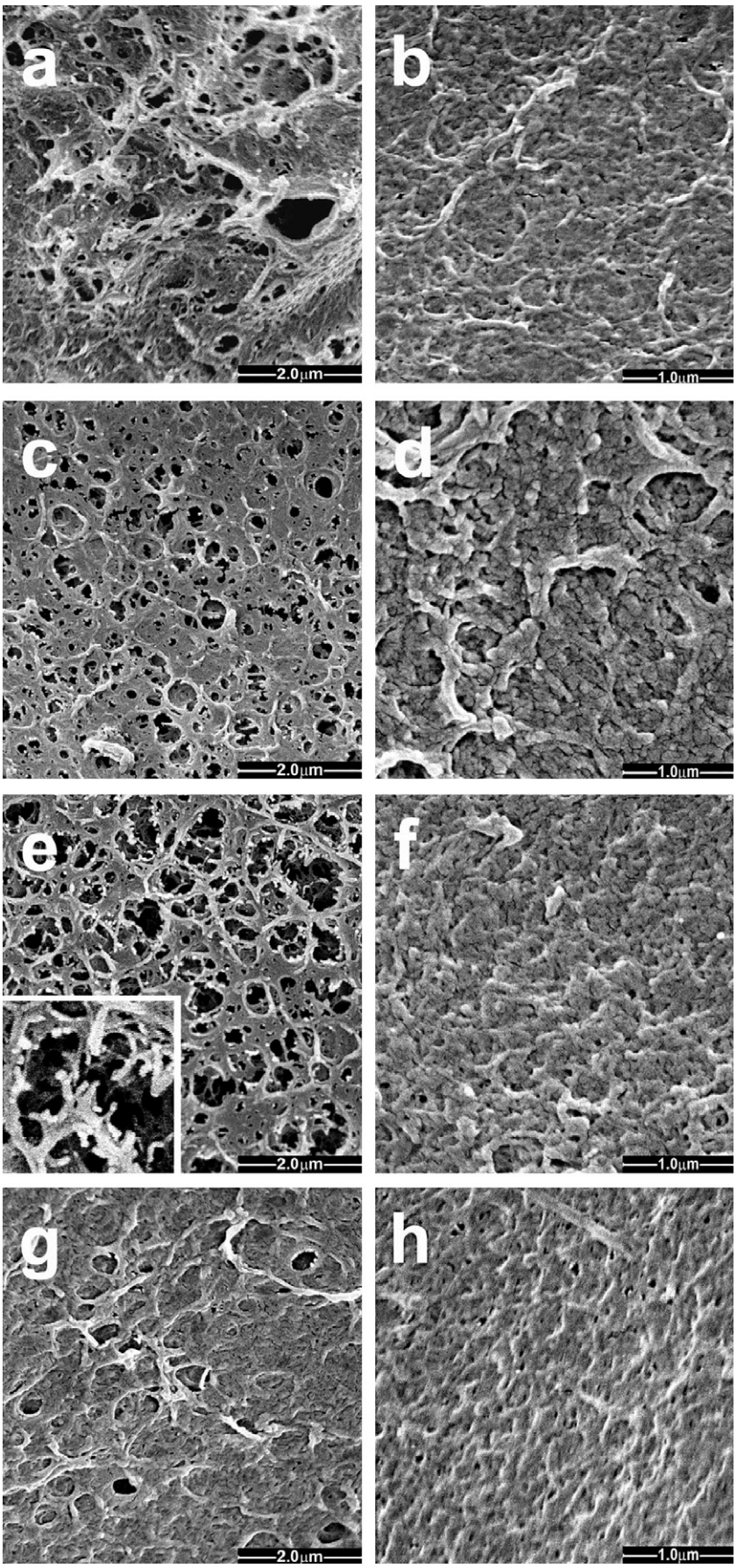

Fig. 4. SEM images of the cross-sections (left) and surfaces (right) of regenerated cellulose gels with different cellulose nanowhiskers contents: 0 (a, b), 20 (c, d), 35 (e, f), and 50 wt% (g, h).

ously decreased diffusion coefficient of CC50 (1.93×10^{-4} mm^2/s).

It is the first time that the nanowhiskers reinforced all-cellulose composite gels are prepare by employing a thermal-induced phase separation process. Compared with other pre-gelation processes, it is a convenient and time-saving method (several minutes) practical for industrial applications. CN played an important role during the whole processing of the all-cellulose composite gel formation. They acted as the "bridge" to facilitate the crosslinking of cellulose chains, promote the diffusion of solvent and nonsolvent molecules, provide a good support to the gel network to maintain a homogeneous shrinkage, and improve the mechanical property of the composite gels.

3.2. All-cellulose composite gel morphology and molecular structures

Fig. 4 shows SEM images of the cross-sections and surfaces of regenerated cellulose gels with different CN contents. The expected more homogeneous porous architectures were observed in CC20 and CC35 than that of CC0. The shrinkage during the regeneration was irregular in CC0 and was controlled by the support of CNs in CC20 and CC35. It was difficult to distinguish CNs or their aggregates on the cross-section of CC20, indicating that CNs were well dispersed and embedded in the regenerated cellulose matrix. When CN content was 35 wt%, pores with tiny branches appeared, as shown in the insert of Fig. 4e. A further increased CN content, regenerated cellulose matrix could not cover all the CNs and some of them were exposed after the shrinkage. It also directly proved the uniformly dispersed CNs caused by "switching off" process at the suspension status, and after regeneration, CNs were still well distributed in the network. However, much fewer pores existed on the cross-section of CC50. That was because a more jammed hydrogen bonded network formed in CC50 and the distance between CNs was much closer than those in other suspensions, as shown in the rheological tests. Thus, CNs combined together to come into the phase continuity and blocked the pores during the regeneration. Interestingly, similar dense surfaces, which demonstrated the same appearance as porous membranes, were observed in all the samples. It could be explained that a high diffusion rate of the solvent and nonsolvent molecules existed on the surfaces of the gels, leading to a strong shrinkage which was beyond the support of CNs. This observed surface morphology also agrees well with the results of the regeneration kinetic test. In summary, with the addition of CNs, the all-cellulose composite gels prepared in this work demonstrate membrane–matrix hybrid structures, featuring dense surfaces and various porous inside architectures reinforced by CNs.

Hydrogen bonds were considered the main interactions in the physical crosslinked all-cellulose composite gels. Therefore, the infrared spectrometer, which is known as a powerful instrument for the investigation of hydrogen bonding behavior and cellulose crystalline structure (Kataoka & Kondo, 1998; Kondo, Koschella, Heublein, Klemm, & Heinze, 2008), was employed to study the regenerated gels. The FT-IR spectra of cellulose gels and neat CN powder are shown in Fig. 5. CN was proved to be cellulose I crystalline by X-ray diffraction (Wang, Tian, et al., 2010), which is thermo-dynamically stable and prevails in cotton and tunicate cellulose, and shows the absorbance of the bands at 3344 and 710 cm^{-1} (Åkerholm, Hinterstoisser, & Salmén, 2004; Azizi Samir, Alloin, & Dufresne, 2005; Oh, Yoo, Shin, Kim, et al., 2005; Sugiyama, Persson, & Chanzy, 1991). The absorbance of the band at 1430 cm^{-1} also corresponds to a crystalline absorption and is closely related to the portion of cellulose I structure (Oh, Yoo, Shin, & Seo, 2005). When CN content was 20 wt%, the absorbance of the bands at 1430 and 710 cm^{-1} was very weak, indicating that CNs (cellulose I) were dispersed and embedded in the regenerated cellulose matrix

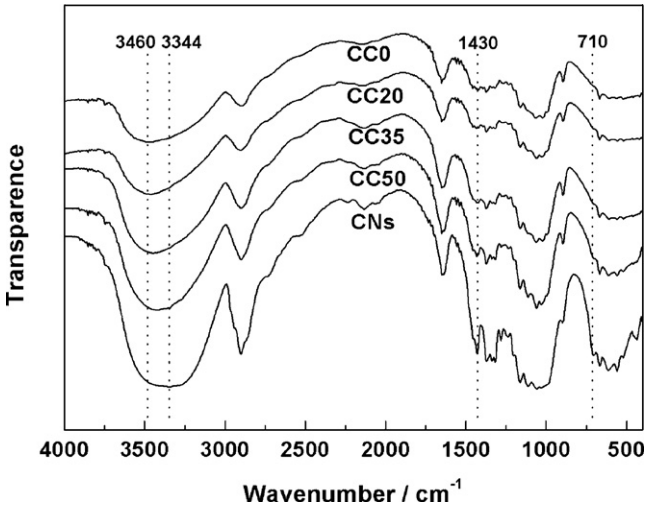

Fig. 5. FT-IR spectra of regenerated cellulose gels having different cellulose nanowhiskers contents and neat cellulose nanowhisker powder.

(cellulose II) by "switching off and on" the inter-particle hydrogen bonding interactions, which was observed by SEM. With the further increase of CN content, CNs were exposed and gradually formed the continued phase, resulting in the increased intensity of the peaks at 1430 and 710 cm^{-1}. The addition of CNs might disturb the origin interactions existed in neat cellulose gel and affect the formation of regenerated cellulose crystal. For CC0 sample, the hydrogen bonded –OH groups stretching vibration exhibited a strong absorption peak centered at 3460 cm^{-1}. This absorption peak gradually shifted to lower wavenumbers at 3417 cm^{-1} and its intensity increased with the higher CN content, confirming that a stronger and denser hydrogen bonded network formed in the all-cellulose composite gels when CNs acted as the crosslinking point and scaffold.

3.3. All-cellulose composite gel properties

3.3.1. Mechanical performance

The mechanical performance of the regenerated cellulose gels was evaluated under compression, and the stress–strain curves are shown in Fig. 6. The neo-Hookean constitutive relationship for rubbers was utilized to analyze the data. In this model, an expression for stress (σ) is derived as the following equation (Sanabria-DeLong,

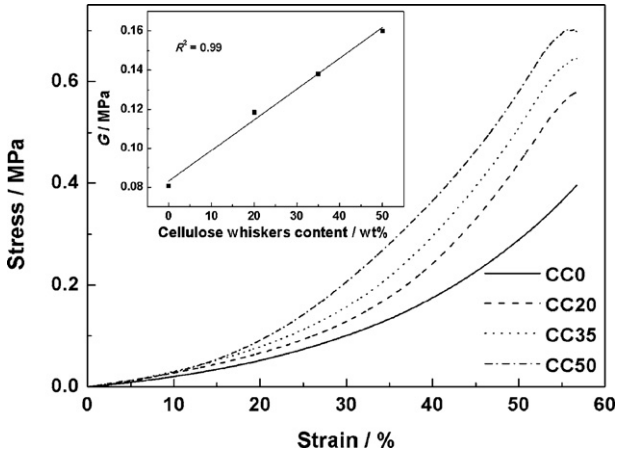

Fig. 6. Stress–strain curves of regenerated cellulose gels having different cellulose nanowhiskers contents. *Inset*: Shear modulus with varying cellulose nanowhiskers contents.

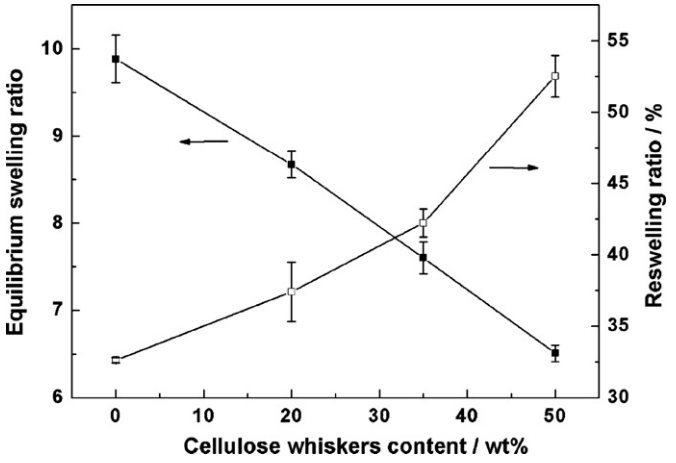

Fig. 7. Swelling and re-swelling properties of regenerated cellulose gels with different cellulose nanowhiskers contents.

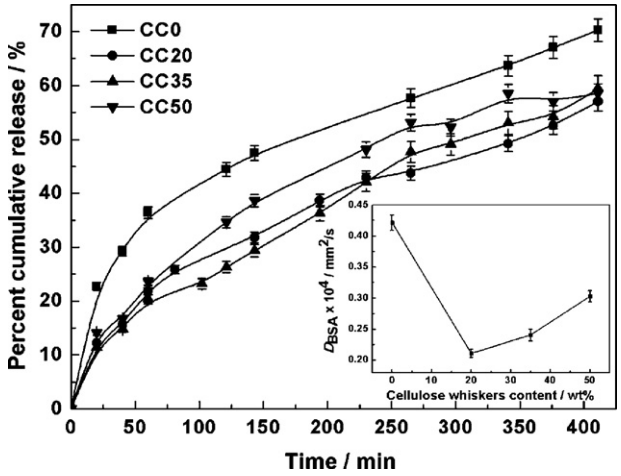

Fig. 8. Release profiles of bovine serum albumin from drug-loaded cellulose gels with different cellulose nanowhiskers contents in simulated body fluid at 37 °C. *Inset*: Diffusion coefficients with varying cellulose nanowhiskers contents.

Crosby, & Tew, 2008):

$$\sigma = 2C_1\left[(\varepsilon+1) - \frac{1}{(\varepsilon+1)^2}\right] \quad (10)$$

where ε is the strain, and the single parameter C_1 is defined as half of the shear modulus, G ($C_1 = G/2$). It was found that the fit was in excellent agreement with the stress–strain curves and predicted the observed nonlinear behavior well ($R^2 = 0.99$), suggesting that the regenerated gels were a rubbery material. By using the neo-Hookean fit, the shear modulus of the regenerated cellulose gels was calculated and plotted in the insert of Fig. 6. With the increase of CN contents, the shear modulus of the neat cellulose gel increased from 81 to 160 kPa, while a much strengthened stress was also observed, indicating an obvious reinforcing effect. There was a linear dependence of shear modulus on the CN concentration. This effect could be explained based on the understanding of the composite gel structure. As already described, CNs were dispersed and acted as the crosslinking points in the gel network to form the jammed hydrogen bonded architecture. If it is assumed that CNs were well-dispersed and all of them contributed to the network, then the crosslinks would be linearly increased. Because the modulus was directly proportional to the crosslink density, the linear relationship between the modulus and the CN content further confirms that CNs were satisfactorily "switched off" and well dispersed in the regenerated cellulose matrix, while were "switched on" during gel thermal treatment and regeneration process, leading to the homogeneous distribution of the CNs in gel matrices to render a better reinforcement (Sanabria-DeLong et al., 2008). All-cellulose gels prepared in this work exhibited similar modulus compared to those of PLA-PEO-PLA hydrogels and PLA-fibrin gels which had been proposed to be used as cartilage tissue engineering materials (Sanabria-DeLong et al., 2008; Zhao, Ma, Gong, Gao, & Shen, 2009). Thus, these elastic natural polymer gels have potential to be used in the biomedical field.

3.3.2. Swelling and re-swelling

A good understanding of gel swelling and re-swelling behaviors is important to evaluate their applications. Fig. 7 shows the swelling and re-swelling properties of the regenerated gels with different CN contents. All gel samples had relatively strong water-holding capacity. The equilibrium swelling ratio (*ESR*) of the gels was impacted by CN content in the gel matrices: with CN content increasing from 0 to 50 wt%, *ESR* values of the composite gels gradually decreased from 9.88 to 6.50. This is due to the increased crosslinking density which restricted the swelling of regenerated cellulose matrix. The gels were then freeze-dried for testing their re-swelling property. When immersed in water bath, dried gels swelled to different extents depending on their CNs content. The composite gels containing more CNs showed higher re-swelling ratios. This may be explained since a stiffer network was formed at high CN content, which could prevent further crosslinking of the cellulose chains during the drying processing and were propitious to the water uptake.

3.3.3. Release property

The release behaviors of the composite gels were subsequently investigated, and bovine serum albumin (BSA) was employed as a model molecule. The BSA loading in the gels are around 11.19–13.81 mg/g. Fig. 8 shows the release profiles of BSA in simulated body fluid (SBF) at 37 °C. The amounts of the drugs released at equilibrium, M_∞, were tested after incubating for 48 h. The release profile of CC0 gel could be modelled according to first-order kinetics ($R^2 = 0.99$). It showed a burst release and about 36% of the loaded drug was detected in the release medium in the first 60 min. This initial burst release is not favorable to sustained or controlled release from a pharmaceutical viewpoint, because it not only wastes the release agent but also shortens the long-term therapeutic effect (Zhao, Platt, & Xie, 2009). Interestingly, the addition of CNs modified BSA release profiles. BSA molecules were steadily released form CC20, CC35 and CC50 gels during the test. The release rates followed a near zero-order kinetics ($R^2 = 0.98$) after 20 min of the test. Moreover, the release of BSA from the composite gels was proportional to the square root of time (M_t/M_∞ versus $t^{1/2}$, $R^2 = 0.99$), indicating that the hydrogels served as diffusion barriers and the proteins were released through Fickian diffusion mechanism. The diffusion coefficients were calculated and plotted in the inserts of Fig. 8. The diffusion coefficient of the composite gels decreased dramatically from 0.42×10^{-4} to 0.21×10^{-4} mm^2/s with the CN content increased from 0 to 20 wt%, and then raised gradually to 0.30×10^{-4} mm^2/s when the CN content was 50 wt%. As observed by SEM, some irregular big pores existed in CC0. This anomalous structure could be a major reason for the burst release phenomenon. Whereas CNs reinforced cellulose gels showed rather homogeneous porous structures, thus the burst release could be avoided and a near zero-release kinetics was obtained. For CC50, CNs combined together and blocked some pores in the gel, so it might be difficult for BSA to penetrate into the inside of the composite gel during the drug loading process, leading to a higher BSA

loading at the matrix surface and consequently a slightly increased diffusion coefficient. The release results showed that CNs could impact the morphology of cellulose gels, subsequently their diffusion properties. Steadily release of BSA could be achieved by addition of CNs in the cellulose gel systems.

4. Conclusions

In this work, nanowhiskers reinforced all-cellulose composite gels were prepared through a convenient and time-saving process involving a rapid thermal-induced phase separation followed by a regenerating process. Cellulose nanowhiskers played important roles to promote cellulose gelation and increased the dimensional stability of gel systems during the regeneration. In the presence of cellulose nanowhiskers, the composite gels exhibited dense surfaces and well-organized porous inside structures as well as significantly enhanced mechanical properties. Moreover, these composite gels demonstrated capacity to steadily release BSA in the simulated body fluid. Therefore, these novel nanocomposite gels may have potential applications in bioengineering and biomedical areas.

Acknowledgments

The authors are grateful to the Natural Sciences and Engineering Research Council of Canada (NSERC), Alberta Barley Commission, Alberta Crop Industry Development Fund Ltd. (ACIDF) and Alberta Innovates-Bio Solutions (AI-Bio) for financial support.

References

Andrews, G. P., Gorman, S. P., & Jones, D. S. (2005). Rheological characterization of primary and binary interactive bioadhesive gels composed of cellulose derivatives designed as ophthalmic viscosurgical devices. *Biomaterials*, *26*, 571–580.

Åkerholm, M., Hinterstoisser, B., & Salmén, L. (2004). Characterization of the crystalline structure of cellulose using static and dynamic FT-IR spectroscopy. *Carbohydrate Research*, *339*, 569–578.

Azizi Samir, M. A. S., Alloin, F., & Dufresne, A. (2005). Review of recent research into cellulosic whiskers, their properties and their application in nanocomposite field. *Biomacromolecules*, *6*, 612–626.

Biganska, O., & Navard, P. (2005). Kinetics of precipitation of cellulose from cellulose-NMMO-water solutions. *Biomacromolecules*, *6*, 1948–1953.

Bingöl, B., Strandberg, C., Szabo, A., & Wegner, G. (2008). Copolymers and hydrogels based on vinylphosphonic acid. *Macromolecules*, *41*, 2785–2790.

Cai, J., & Zhang, L. (2005). Rapid dissolution of cellulose in LiOH/urea and NaOH/urea aqueous solutions. *Macromolecular Bioscience*, *5*, 539–548.

Cai, J., Liu, Y., & Zhang, L. (2006). Dilute solution properties of cellulose in LiOH/urea aqueous system. *Journal of Polymer Science Part B Polymer Physics*, *44*, 3093–3101.

Cai, J., & Zhang, L. (2006). Unique gelation behavior of cellulose in NaOH/urea aqueous solution. *Biomacromolecules*, *7*, 183–189.

Cai, J., Zhang, L., Zhou, J., Qi, H., Chen, H., Kondo, T., et al. (2007). Multifilament fibers based on dissolution of cellulose in NaOH/urea aqueous solution: structure and properties. *Advanced Materials*, *19*, 821–825.

Capadona, J. R., van den Berg, O., Capadona, L., Schroeter, M., Tyler, D., Rowan, S. J., & Weder, C. (2007). A versatile approach for the processing of polymer nanocomposites with self-assembled nanofiber templates. *Nature Nanotechnology*, *2*, 765–769.

Capadona, J. R., Shanmuganathan, K., Tyler, D. J., Rowan, S. J., & Weder, C. (2008). Stimuli-responsive polymer nanocomposites inspired by the sea cucumber dermis. *Science*, *319*, 1370–1374.

Capadona, J. R., Shanmuganathan, K., Trittschuh, S., Seidel, S., Rowan, S. J., & Weder, C. (2009). Polymer nanocomposites with nanowhiskers isolated from microcrystalline cellulose. *Biomacromolecules*, *10*, 712–716.

Chang, C., Lue, A., & Zhang, L. (2008). Effects of crosslinking methods on structure and properties of cellulose/PVA hydrogels. *Macromolecular Chemistry and Physics*, *209*, 1266–1273.

Chen, Y., Liu, C., Chang, P. R., Cao, X., & Anderson, D. P. (2009). Bionanocomposites based on pea starch and cellulose nanowhiskers hydrolyzed from pea hull fibre: Effect of hydrolysis time. *Carbohydrate Polymers*, *76*, 607–615.

Entcheva, E., Bien, H., Yin, L., Dhung, C. Y., Farell, M., & Kostov, Y. (2004). Functional cadiac cell constructs on cellulose-based scaffolding. *Biomaterials*, *25*, 5753–5762.

Fundueanu, G., Constantin, M., Esposito, E., Cortesi, R., Nastruzzi, C., & Menegatti, E. (2005). Cellulose acetate butyrate microcapsules containing dextran ion-exchange resins as self-propelled drug release system. *Biomaterials*, *26*, 4337–4347.

Gavillon, R., & Budtova, T. (2007). Kinetics of cellulose regeneration from cellulose-NaOH-water gels and comparison with cellulose-N-methylmorpholine-N-oxide-water solutions. *Biomacromolecules*, *8*, 424–432.

Hoepfner, S., Ratke, L., & Milow, B. (2008). Synthesis and characterization of nanofibrillar cellulose aerogels. *Cellulose*, *15*, 121–129.

Kataoka, Y., & Kondo, T. (1998). FT-IR microscopic analysis of changing cellulose crystalline structure during wood cell wall formation. *Macromolecules*, *31*, 760–764.

Klemm, D., Schumann, D., Udhardt, U., & Marsch, S. (2001). Bacterial synthesized cellulose-artificial blood vessels for microsurgery. *Progress in Polymer Science*, *26*, 1561–1603.

Klemm, D., Heublein, B., Fink, H. P., & Bohn, A. (2005). Cellulose: Fascinating biopolymer and sustainable raw material. *Angewandte Chemie International Edition*, *44*, 3358–3393.

Kokubo, T., & Takadama, H. (2006). How useful is SBF in predicting in vivo bone bioactivity? *Biomaterials*, *27*, 2907–2915.

Kondo, T., Koschella, A., Heublein, B., Klemm, D., & Heinze, T. (2008). Hydrogen bond formation in regioselectively functionalized 3-mono-O-methyl cellulose. *Carbohydrate Research*, *343*, 2600–2604.

Liang, S., Zhang, L., Li, Y., & Xu, J. (2007). Fabrication and properties of cellulose hydrated membrane with unique structure. *Macromolecular Chemistry and Physics*, *208*, 594–602.

Liang, S., Wu, J., Tian, H., Zhang, L., & Xu, J. (2008). High-strength cellulose/poly(ethylene glycol) gels. *ChemSusChem*, *1*, 558–563.

Lu, Y., Weng, L., & Cao, X. (2006). Morphological, thermal and mechanical properties of ramie crystallites-reinforced plasticized starch biocomposites. *Carbohydrate Polymers*, *63*, 198–204.

Luo, X., Liu, S., Zhou, J., & Zhang, L. (2009). In situ synthesis of Fe_3O_4/cellulose microspheres with magnetic-induced protein delivery. *Journal of Materials Chemistry*, *19*, 3538–3545.

Nguyen, K. T., & West, J. L. (2002). Photopolymerizable hydrogels for tissue engineering applications. *Biomaterials*, *23*, 4307–4314.

Oh, S. Y., Yoo, D. I., Shin, Y., Kim, H. C., Kim, H. Y., Chung, Y. S., et al. (2005). Crystalline structure analysis of cellulose treated with sodium hydroxide and carbon dioxide by means of X-ray diffraction and FTIR spectroscopy. *Carbohydrate Research*, *340*, 2376–2391.

Oh, S. Y., Yoo, D. I., Shin, Y., & Seo, G. (2005). FTIR analysis of cellulose treated with sodium hydroxide and carbon dioxide. *Carbohydrate Research*, *340*, 417–428.

Paralikar, S. A., Simonsen, J., & Lombardi, J. (2008). Poly(vnyl alcohol)/cellulose nanocrystals barrier membranes. *Journal of Membrane Science*, *320*, 248–258.

Qi, H., Cai, J., Zhang, L., & Kuga, S. (2009). Properties of films composed of cellulose nanowhiskers and a cellulose matrix regenerated from alkali/urea solution. *Biomacromolecules*, *10*, 1597–1602.

Roohani, M., Habibi, Y., Belgacem, N. M., Ebrahim, G., Karimi, A. N., & Dufresne, A. (2008). Cellulose whiskers reinforced polyvinyl alcohol copolymers nanocomposites. *European Polymer Journal*, *44*, 2489–2498.

Ruan, D., Lue, A., & Zhang, L. (2008). Gelation behaviors of cellulose solution dissolved in aqueous NaOH/thiourea at low temperature. *Polymer*, *49*, 1027–1036.

Sahiner, N., Singh, M., Kee, D. D., John, V. T., & McPherson, G. L. (2006). Rheological characterization of a charged cationic hydrogel network across the gelation boundary. *Polymer*, *47*, 1124–1131.

Sanabria-DeLong, N., Crosby, A. J., & Tew, G. N. (2008). Photo-cross-linked PLA-PEO-PLA hydrogels from self-assembled physical networks: mechanical properties and influence of assumed constitutive relationships. *Biomacromolecules*, *9*, 2784–2791.

Sescousse, R., & Budtova, T. (2009). Influence of processing parameters on regeneration kinetics and morphology of porous cellulose from cellulose-NaOH-water solutions. *Cellulose*, *16*, 417–426.

Shanmuganathan, K., Capadona, J. R., Rowan, S. J., & Weder, C. (2010). Bio-inspired mechanically-adaptive nanocomposites derived from cotton cellulose whiskers. *Journal of Materials Chemistry*, *20*, 180–186.

Singh, B. (2007). Psyllium as therapeutic and drug delivery agent. *International Journal of Pharmaceutics*, *334*, 1–14.

Sugiyama, J., Persson, J., & Chanzy, H. (1991). Combined infrared and electron diffraction study of the polymorphism of native celluloses. *Macromolecules*, *24*, 2461–2466.

Wang, Y., & Zhang, L. (2008). High-strength waterborne polyurethane reinforced with waxy maize starch nanocrystals. *Journal of Nanoscience and Nanotechnology*, *8*, 5831–5838.

Wang, Y., Chang, C., & Zhang, L. (2010). Effects of freezing/thawing cycles and cellulose nanowhiskers on structure and properties of biocompatible starch/PVA sponges. *Macromolecular Materials and Engineering*, *295*, 137–145.

Wang, Y., Tian, H., & Zhang, L. (2010). Role of starch nanocrystals and cellulose whiskers in synergistic reinforcement of waterborne polyurethane. *Carbohydrate Polymer*, *80*, 665–671.

Weng, L., Zhang, L., Ruan, D., Shi, L., & Xu, J. (2004). Thermal gelation of cellulose in a NaOH/thiourea aqueous solution. *Langmuir*, *20*, 2086–2093.

Wu, J., Liang, S., Dai, H., Zhang, X., Yu, X., Cai, Y., et al. (2010). Structure and properties of cellulose/chitin blended hydrogel membranes fabricated via a solution pregelation technique. *Carbohydrate Polymers*, *79*, 677–684.

Zhang, H., Wang, Z., Zhang, Z., Wu, H., Zhang, J., & He, J. (2007). Regenerated-cellulose/multiwalled-carbon-nanotube composite fibers

with enhanced mechanical properties prepared with the ionic liquid 1-allyl-3-methylimidazolium chloride. *Advanced Materials*, *19*, 698–704.

Zhao, H., Ma, L., Gong, Y., Gao, C., & Shen, J. (2009). A polylactide/fibrin gel composite scaffold for cartilage tissue engineering: fabrication and an in vitro evaluation. *Journal of Materials Science: Materials in Medicine*, *20*, 135–143.

Zhao, J., Platt, J. A., & Xie, D. (2009). Characterization of a novel light-cured star-shape poly(acrylic acid)-composed glass-ionomer cement: fluoride release, water sorption, shrinkage, and hygroscopic expansion. *European Journal of Oral Sciences*, *117*, 755–765.

Zhou, J., Chang, C., Zhang, R., & Zhang, L. (2007). Hydrogels prepared from unsubstituted cellulose in NaOH/urea aqueous solution. *Macromolecular Bioscience*, *7*, 804–809.